

https://doi.org/10.1070/QEL17370

Effect of finite ion mass on relativistic self-induced transparency of plasma layers with a sharp boundary

N.A. Mikheitsev, A.V. Korzhimanov

Abstract. **We consider the effect of ion mobility on the threshold of relativistic self-induced transparency under irradiation of thin plasma layers by circularly polarised laser radiation. An analytical model of the motion of ions during the removal of electrons from the layer surface by the ponderomotive force of laser radiation is constructed. The model is used to analyse the motion of probe electrons in the resulting electromagnetic field. It is shown that the higher the ion mobility and the longer the laser pulse, the more stable the plasma layer to longitudinal perturbations of a finite value and the higher the threshold of self-induced transparency. These conclusions are verified by one-dimensional numerical simulation of a complete system of kinetic equations for plasma and Maxwell's equations.**

Keywords: *relativistic laser plasma, relativistic self-induced transparency, laser acceleration of ions, multiply charged ions, petawatt lasers.*

1. Introduction

To date, the development of technologies for producing pico- and femtosecond ultrahigh-power laser pulses has led to the fabrication of systems with a peak radiation power of several petawatts [1–3]. Focusing such radiation into a spot whose diameter corresponds to a diffraction limit (~1–2 μm) allows one to achieve a radiation intensity exceeding 10^{22} W cm^{-2}, while the use of an intensity of about 10^{21} W cm^{-2} and higher is currently relatively routine for experiments. In particular, such intensities are characteristic of the problems of acceleration of protons [4–8] and rather heavy ions [9], creation of a high-energy-density substance [10, 11], and also of the generation of multiply charged ions [12], bright gamma radiation [13, 14] and high-density electron–positron fluxes [15]. In most of these applications, we speak of the interaction with solid-state targets that have a supercritical density at the moment of ionisation. Usually, the use of targets with near-critical density improves the interaction efficiency and is optimal; for example, ion acceleration using such targets has been previously demonstrated in [16–21] (see also reviews [22–24]).

N.A. Mikheitsev Lobachevsky State University of Nizhny Novgorod, prosp. Gagarina 23, 603950 Nizhny Novgorod, Russia;
A.V. Korzhimanov Institute of Applied Physics, Russian Academy of Sciences, ul. Ulyanova 46, 603950 Nizhny Novgorod, Russia;
e-mail: artem.korzhimanov@ipfran.ru

Received 18 May 2020
Kvantovaya Elektronika **50** (8) 776–781 (2020)
Translated by I.A. Ulitkin

In this regard, of particular importance is the correct determination of the threshold of relativistic self-induced transparency (RSIT). This effect was first described more than half a century ago by the example of a monochromatic plane wave propagating in an infinite homogeneous plasma [25]. In this approximation, the plasma is transparent when the condition

$$a > a_{\rm th} = \sqrt{n_0^2 - 1} \tag{1}$$

is met, where $a = e\mathcal{E}/(m\omega c)$ is the dimensionless amplitude of the laser pulse; $\mathcal{E}$ and ω are the amplitude and frequency of the electromagnetic wave, respectively; e is the elementary charge; m is the mass of the electron; $n_0 = N_{\rm e0}/N_{\rm c} = 4\pi e^2 N_{\rm e0}/(m\omega^2)$ is the plasma overdense parameter; $N_{\rm e0}$ is the unperturbed density of electrons in the plasma; and $N_{\rm c}$ is the critical density. When considering a practically more interesting case of irradiation of a semi-bounded plasma layer, the transparency threshold is generally the same [26], with the exception, at least, of a sharp boundary irradiated along the normal by a circularly polarised pulse [27]. In the latter case, the interaction of laser radiation with matter is observed only in the skin layer of subwavelength thickness, and due to the use of circular polarisation, there is no effective heating of electrons; as a result, their temperature remains much lower than the relativistic one [28]. These two circumstances lead to a significant increase in the influence of striction nonlinearity associated with a local change in the electron density under the action of the ponderomotive force from the electromagnetic field. As a result, the RSIT threshold $a_{\rm th}$ increases. As was shown in [27], for the idealised case of negligible electron temperature and stationary ions, the threshold is expressed as

$$a_{\rm th} = \frac{1}{2}\left[\frac{2}{3}(1 + a_{\rm d}^2)(2a_{\rm d}^2 - n_0) - a_{\rm d}^4\right]^{1/2}, \tag{2}$$

where

$$a_{\rm d}^2 = n_0\left(\frac{9}{8}n_0 - 1 + \frac{3}{2}\sqrt{\frac{9}{16}n_0^2 - n_0 + 1}\right). \tag{3}$$

In the ultrarelativistic limit reached at $n_0 \gg 1$, this expression can be simplified:

$$a_{\rm th} \approx \frac{3\sqrt{3}}{8}n_0^2. \tag{4}$$

It follows from this expression that the threshold in this case increases with increasing plasma density much faster than according to the classical dependence (1). This property was

used in [17, 20] to increase the efficiency of laser-plasma acceleration of protons.

The threshold given by expression (2) was obtained under fairly strong assumptions and requires correction when, for example, the finite electron temperature and ion mobility are taken into account. In particular, as was shown in [28], the presence of a longitudinal spread in electron velocities leads to an inevitable escape of part of the high-energy electrons towards the radiation and the concomitant penetration of the radiation deep into the plasma. This escape is absent or negligible for a small spread, but becomes significant for a large one. At a certain threshold longitudinal electron temperature, the dynamics of the interaction of laser radiation with plasma becomes practically indistinguishable from the RSIT dynamics described in [29]. Thus, this temperature or the corresponding longitudinal momentum can also be considered as the RSIT threshold.

The threshold longitudinal momentum depends on the distribution of potentials near the boundary of the electron layer and, in particular, on the distribution of the ionic component. It was assumed in [28] that the ions are motionless, but this assumption is true only if the laser pulse duration is sufficiently short compared to the inverse ion plasma frequency: $\tau_L \ll \omega_{pi}^{-1} = (4\pi Z^2 e^2 N_i/M)^{-1/2}$, where Z, M, and N_i are the ionisation yield, ion mass and ion density, respectively. Even for targets with near-critical density, for which the electron plasma frequency $\omega_{pe} \approx \omega$, this condition can be violated even for relatively short laser pulses. Indeed, $\omega_{pi} = \omega_{pe}(Zm/M)^{1/2} \approx \omega(Zm/M)^{1/2}$, while the ratio $(Zm/M)^{-1/2} \approx 40$ for protons and due to deep optical ionisation is only two to three times greater even for the most heavy ions. Therefore, the stationary-ion approximation is no longer fulfilled for pulses of about 100 fs duration, and in the case of denser targets, the approximation is not met even for shorter pulses. Thus, in many practically important cases, it is necessary to take into account the motion of ions.

Such an account, from the point of view of its influence on the RSIT threshold, was performed in [30]. It was shown that the redistribution of the ion component causes an increase in the threshold longitudinal momentum. However, in [30], the analysis was performed only for the case of a semi-infinite plasma layer in which the ions are accelerated in the snowplow or hole-boring regime. In the present work, we also study an interesting case of thin plasma layers in which 'light sail' ion acceleration is possible.

The paper is structured as follows. Section 2 presents an analytical method for solving the hydrodynamic equations of motion for the ion component in the process of removal of the electron layer from the layer surface by a laser pulse with a given envelope. In Section 3, we analyse the motion of probe electrons with a nonzero longitudinal momentum in quasi-stationary laser-plasma structures with allowance for the redistribution of the ion component. Based on this analysis, we determine the dependence of the threshold value of the longitudinal momentum at which the electron leaves the layer on the laser pulse amplitude and duration, as well as on the target density and the ion charge/mass ratio. Finally, in Section 4, by means of one-dimensional numerical simulation by the particle-in-cell method, the problem of the bleaching of a thin layer of a supercritical plasma is studied, in which, at some thicknesses, a sharp dependence of the nonlinear reflection coefficient on the ion mass is observed: the layer is transparent in the case of heavy ions and nontransparent in the case of relatively light ions.

2. Analytical model of the motion of ions

Let us consider the incidence of a circularly polarised, plane monochromatic electromagnetic wave onto a thick layer of a homogeneous supercritical plasma along the normal to the layer boundary. We will describe the plasma in the hydrodynamic approximation. Since the characteristic response times of the electron and ion components differ by at least one and a half orders of magnitude, and the characteristic time of the reaction of electrons to an external action is usually much shorter than the characteristic time of a rise in the intensity of the incident laser pulse, the problem can be solved in the approximation of inertialess electrons that at each time moment are in the stationary state determined by the balance of forces acting on them: ponderomotive from the side of the electromagnetic wave and electrostatic associated with the separation of charges. We will also assume that the temperature of the electrons is zero, because it can be neglected in comparison with their oscillatory energy due to the low collision frequency resulting from the relativistic electron velocity and the absence of effective collisionless heating due to the use of circularly polarised radiation incident along the normal. In this case, to construct stationary distributions, one can apply the method described, for example, in [31].

However, for sufficiently large field amplitudes and plasma densities, the problem can be simplified, since, as was shown in [17], in this case the spatial distribution of electrons is a cavity on the irradiated side of the plasma layer, completely devoid of electrons, and a thin electron layer at its boundary. Therefore, we assume that at each moment of time the displaced electrons form an infinitely thin, delta-shaped layer located at some point $z_b(t)$, determined by a simple balance of light pressure and electrostatic force (a more detailed derivation of the formula is given in [32]):

$$\frac{\omega z_b}{c} = \frac{2a(t, z_b)}{n_0}. \tag{5}$$

The equations of motion for ions will be solved in Lagrangian coordinates. We also restrict ourselves to the case of intensities at which the movement of ions in the wave field is not relativistic, which allows us to neglect the ponderomotive force as compared to the electrostatic one. In practice, this means that the pulse intensity should be less than 10^{24} W cm^{-2}, which obviously exceeds the applicability limit of the equations used for electrons due to the absence of radiation losses and the production of electron–positron pairs [33].

Thus, the movement of the ionic liquid will be described by the system of equations:

$$\frac{dz}{dt} = \frac{P}{\Gamma M}, \quad \frac{dP}{dt} = ZeE(t),$$

where $E(t)$ is the longitudinal electric field; P and z are the momentum and coordinate of the Lagrangian element of the ionic liquid; and $\Gamma = [1 + P^2/(Mc)^2)]^{1/2}$ is its Lorentz factor.

A remarkable feature of the system under consideration is that the electric field acting on a certain element of the ionic liquid remains constant for a long time. This is due to the fact that while there is no intersection of the trajectories of the Lagrangian elements in one-dimensional geometry, the integral of the ion density in the range from the layer boundary to a given Lagrangian element remains constant. The intersection of the elements, as follows from the solution of the indi-

cated system and from the numerical simulation of the complete self-consistent system of kinetic equations and Maxwell's equations, can occur over a considerable period of time after the start of interaction and, in addition, violates the applicability condition of the simple single-flow hydrodynamic model. Note that this circumstance has already been noted and used in a slightly different interaction model in [34].

The main difference between the model considered in this paper and the model from [34] is that it takes into account that the motion of ions located at different points in space begins at different moments of time. We will consider this moment of time to be the moment at which the position of the boundary of the removed electrons is compared with the initial position of the Lagrangian element of the ionic liquid.

For further analysis, we assume that the laser pulse amplitude increases linearly and starts from zero at time $t = 0$, then from relation (5), neglecting the delay effect, we obtain that the motion of the boundary of the electron layer is also linear. We introduce the velocity of this motion $V = c2a_i/(n_0\omega\tau)$, where a_i is the laser pulse amplitude at time $t = \tau$. Then the approximation of the absence of delay is valid for $V \ll c$.

In these approximations, the electric field acting on the Lagrangian particle of the ionic liquid, which was at some point z_0 at the initial moment of time, can be written as

$$E(t) = 4\pi ZeN_{i0}z_0\Theta\left(t - \frac{z_0}{V}\right) = \frac{M\omega_{pi0}^2}{Ze}z_0\Theta\left(t - \frac{z_0}{V}\right), \qquad (6)$$

where N_{i0} and ω_{pi0} are the ion density and ionic plasma frequency of the unperturbed plasma, and $\Theta(t)$ is the Heaviside function.

Thus, the system of equations of motion of the ionic liquid takes the form

$$\frac{dz}{dt} = \frac{P}{M[1 + P^2/(Mc)^2]^{1/2}}, \quad \frac{dP}{dt} = M\omega_{pi0}^2 z_0\Theta\left(t - \frac{z_0}{V}\right).$$

We introduce the dimensionless quantities $\zeta = \omega_{pi0}z/c$, $\beta = V/c$, and $\eta = \omega_{pi0}t$ and integrate this system. We obtain the following implicit relationship between the current position of the Lagrangian particle ζ and its initial position ζ_0:

$$(\beta^2 - 1)\zeta_0^3 + 2(\eta - \beta^2\zeta)\zeta_0^2 + (\beta^2\zeta^2 - 2 - \eta^2)\zeta_0 + 2\zeta = 0. \quad (7)$$

Knowing the relationship between the initial and final positions of the liquid layer, it is possible to express the ion density at an arbitrary point in time through the initial density:

$$N_i(\zeta, \eta) = N_{i0}d\zeta_0/d\zeta. \qquad (8)$$

In the general case, equation (7) has three roots. The case, when two roots are complex and one is real, corresponds to single-flow movement. The case of three real roots corresponds to the multi-flow motion, which is beyond the framework of the single-flow hydrodynamic approximation in question.

To verify the adequacy of the analytical model, its results were compared with the results of numerical modelling of a complete self-consistent system of kinetic equations for plasma and Maxwell's equations for electromagnetic fields by the particle-in-cell (PIC) method. Modelling was performed using the Picador software package [35] in one-dimensional geometry. The wavelength of the incident radiation was 1 μm, the length of the computational domain was 3 μm, the spatial

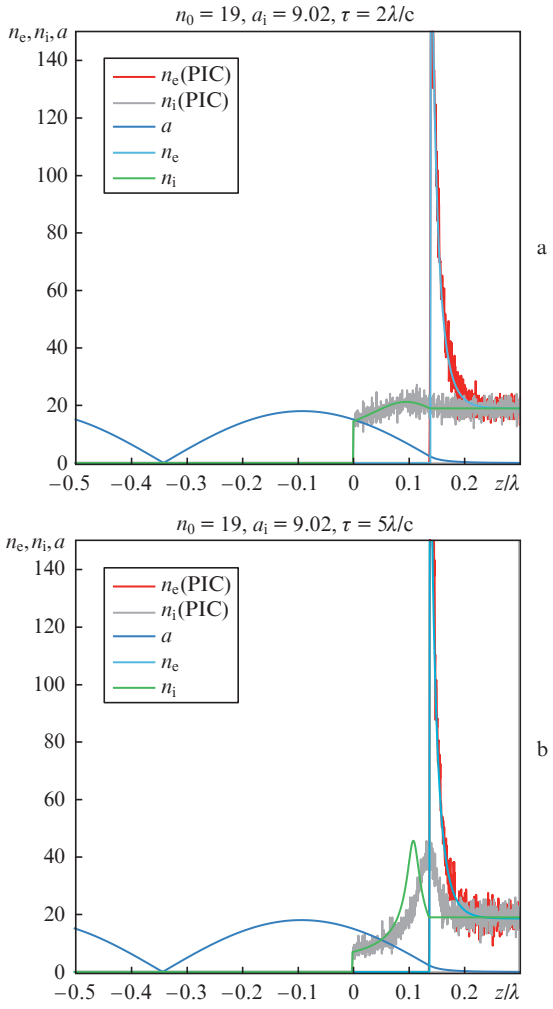

Figure 1. (Colour online) Distributions of fields and densities at various parameters of laser radiation. Here τ is the time of a linear increase in the pulse amplitude from zero to a_i; $n_e = N_e/N_c$; $n_i = N_i/N_c$.

step of the grid was 0.5 nm, and the number of particles in one cell was 30. The results obtained for two sets of pulse and plasma parameters are shown in Fig. 1.

We note a good agreement between the simulation results and the analytical model for relatively short laser pulses. For longer pulses, the simulation results differ from the predictions of the analytical model, which is mainly due to the neglect of the finiteness of the electron layer thickness in it: because of this, the ions begin their motion with a slight delay. Nevertheless, a more detailed comparison showed that the range of durations for which the model is applicable is quite large.

3. Analysis of the motion of probe electrons

Let us now analyse the effect of ion motion on the RSIT threshold. Recall the bleaching mechanism in the case of the incidence of circularly polarised radiation on a sharp boundary of a supercritical plasma along the normal. The ponderomotive force exerted by the laser radiation on the electrons leads to their redistribution and the formation of a quasi-stationary distribution, which is a cavity on the irradiated side of the layer that is completely devoid of electrons and a sharp narrow peak at a point with coordi-

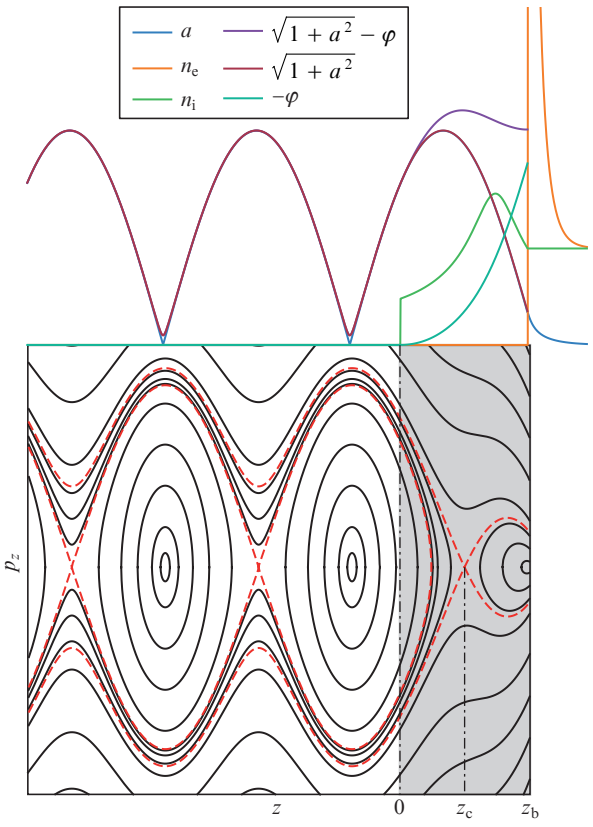

Figure 2. (Colour online) Phase plane of the longitudinal motion of the probe electron near the boundary of the electron layer. Separatrixes are shown by dashed lines.

nate z_b defined by expression (5). It was previously shown that such a distribution is stable at small longitudinal perturbations in the entire region of its existence [28, 29]. This is explained by the fact that in the region without electrons there is a barrier formed by ponderomotive and electrostatic potentials. Loss of stability is possible either when the amplitude reaches a certain threshold value [29], which leads to the disappearance of the barrier, or in the presence of perturbations of a finite value [28], which causes the emergence of electrons with an energy exceeding the height of the barrier. However, in both cases, the scenario of stability loss is the same. A significant part of the electrons flies towards the laser radiation, which leads to a decrease in the number of electrons reflecting the radiation, which makes it move deeper into the plasma. If at the same time the plasma layer has a finite thickness, then at some point in time the radiation reaches its boundary and passes through the initially transparent layer.

Perturbations of a finite value are associated with the presence of a longitudinal momentum in the electrons and can be caused either by their collisionless heating, which, although ineffective for circularly polarised pulses, is nevertheless present, or by the excitation of longitudinal oscillations due to the nonstationary behaviour of the electron removal process.

To determine at which characteristic longitudinal momenta of the electrons their movement towards the laser pulse begins, we analyse the dynamics of the probe electrons in stationary structures with allowance for the redistribution of ions in accordance with the model proposed in Section 2.

The Hamiltonian of electron motion has the following form in dimensionless quantities [28]:

$$H(z,p_z)=\sqrt{1+a^2(z)+p_z^2}-\varphi(z), \tag{9}$$

where $\varphi(z)$ is the electrostatic potential normalised to mc^2/e and obtained in our case from the analytical solution of the above-described ion motion problem; and p_z is the longitudinal momentum of the probe electron, normalised to mc.

An example of the corresponding phase portrait is shown in Fig. 2. We note that in the region $z > z_b$ all the forces acting

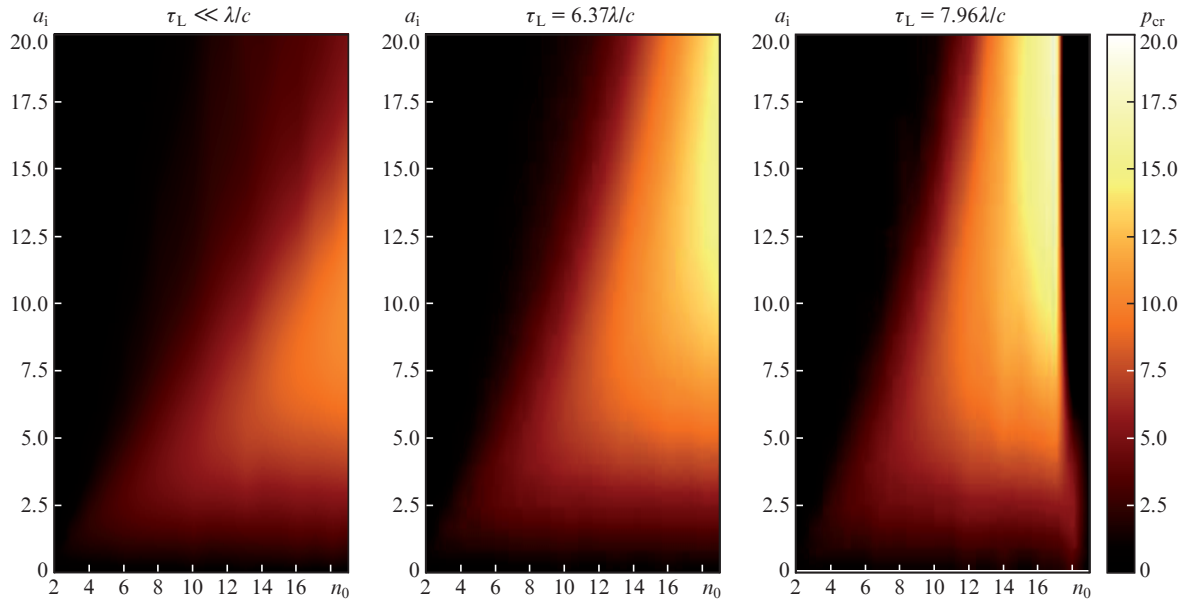

Figure 3. (Colour online) Analytically calculated dependences of the critical momentum on the electron density and the amplitude of the incident field for various incident pulse durations τ_L.

on the electron are precisely compensated for, and therefore it can be omitted. For $z < z_b$, there exists a region of infinite particle motion separated by separatrixes of the saddle nearest to the electron layer boundary. If the electron at the layer boundary has a longitudinal momentum exceeding some critical momentum p_{cr}, then it will be outside the separatrixes and will not return to the plasma layer. Therefore, the magnitude of this critical momentum can be considered a characteristic threshold value for the onset of the RSIT regime.

The critical longitudinal momentum is determined by the position of the saddle and is related to it by the expression following from the constancy of the Hamiltonian along the separatrix:

$$p_{cr}^2 = \left[\sqrt{1 + a^2(z_c)} - \varphi(z_c) + \varphi(z_b)\right]^2 - 1 - a^2(z_b), \qquad (10)$$

where z_c is the position of the nearest saddle to the electron layer boundary.

When the movement of ions is taken into account, particles are redistributed, resulting in a decrease in the electrostatic potential difference. This leads to the fact that the degree of electron stability at the layer boundary increases for targets with lower ion masses and in the case of longer incident pulses. This can be clearly seen from Fig. 3, which shows the dependences of the critical momentum calculated in the framework of the proposed model on the laser pulse amplitude and plasma density for three pulse durations τ_L with an envelope in the form of an isosceles triangle. Note that for the largest of them, for $n_0 > 17$, it is impossible to construct an analytical solution, since the single-flow condition is violated in this region of parameters.

4. Transparency in numerical simulation

An analysis of Fig. 3 shows that reaching the RSIT threshold requires relativistic values of the longitudinal momentum of electrons at the layer boundary, but, as mentioned above, heating is usually small for circular polarisation. Nevertheless, significant longitudinal heating can be observed in plasma layers, the thickness of which is comparable with the value of removal of electrons in them from the layer surface. Indeed, in this case, all the electrons of the layer are compressed into an ultrathin layer. This compression should lead to a substantial heating of electrons in the layer. In addition, the electrons can acquire a significant longitudinal momentum in a substantially non-stationary regime of removal, which takes place at $a_i/n_0 \approx 1$, when the velocity of movement of the electron layer boundary approaches the speed of light. We show that in this case the transparency of the plasma layer can substantially depend on the mass of ions in it.

It is well known that plasma layers whose thickness L is less than some critical value determined by the ratio $\omega L/c = 2a/n_0$ are transparent to radiation, because the electrons in them are completely removed into a layer with a thickness less than the thickness of the skin layer [36, 37]. Figure 4 shows the dependence of the transparency coefficient of such a layer on its thickness in the case when it consists of protons; the dependence is obtained in the process of numerical simulation by the PIC method. The parameters used in the simulation are as follows: $n_0 = 10$, $a_i = 27.8$, $\tau_L = 3\lambda/c$, the spatial step is 1 nm, and the number of particles in one cell is 300. A characteristic feature is the presence of a critical value of the layer thickness, below which it is bleached.

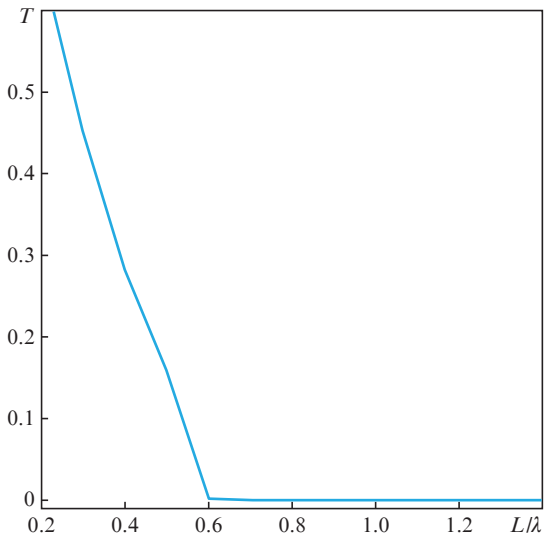

Figure 4. Dependence of the transmission coefficient of the laser pulse, equal to the ratio of the total energy of the transmitted radiation to the energy of the incident pulse through a thin plasma layer consisting of protons, on the thickness of this layer. Parameters of numerical simulation are given in the text.

However, this critical thickness turns out to depend on the mass of ions in the layer and the duration of the laser pulse. Figure 5 shows the dependence of the transparency coefficient on these two values. In these calculations, the layer thickness was fixed, $\omega L/c = 2$ ($L \approx 0.32$ μm for a wavelength of 1 μm). A characteristic feature is an increase in transparency with decreasing laser pulse duration, with the exception of the region $c\tau_L < L$, where the laser pulse duration becomes comparable with the plasma layer thickness: In this region, the pulse does not have enough time to remove the electrons to

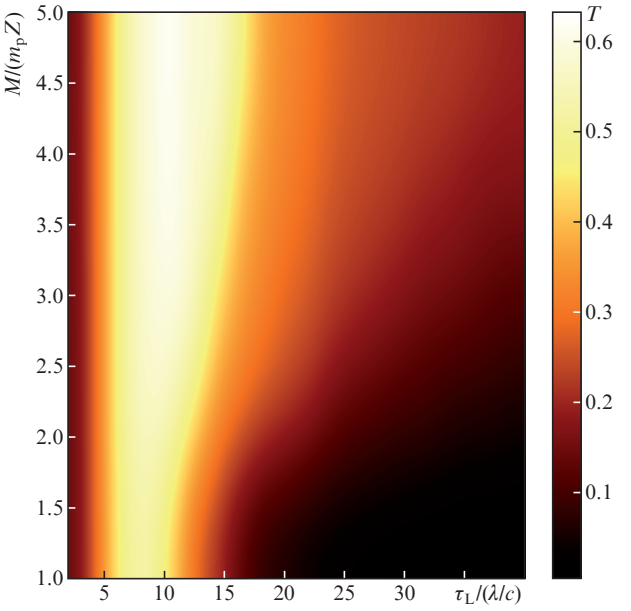

Figure 5. (Colour online) Dependence of the transmission coefficient of the laser pulse through a thin plasma layer on the ratio of the mass of ions to their charge and the duration of the incident pulse (m_p is the mass of the proton).

pass through the layer. In this case, the maximum duration at which transparency is observed decreases with decreasing ion mass, which qualitatively coincides with the conclusion (see Section 3) about greater stability of plasma layers with lighter ions.

5. Conclusions

Thus, we have analysed the effect of ion mobility on the RSIT threshold, which is determined by collisionless longitudinal heating of electrons and the excitation of longitudinal oscillations due to the non-stationary process of electrons' removal from the layer surface in thin plasma layers with a near-critical density. An analytical model of the motion of ions has been constructed, on the basis of which a critical longitudinal momentum of electrons is determined, at which they escape towards the laser radiation, accompanied by the penetration of radiation into the bulk of the plasma. It is shown that the transparency threshold decreases with increasing ion mass and decreasing laser pulse duration.

Based on the analysis performed, we have predicted the dependence of the transparency coefficient of thin plasma layers on the mass of their constituent ions and the duration of the irradiating laser pulse. This dependence is qualitatively confirmed by one-dimensional numerical kinetic simulation, during which we have demonstrated the possibility of a transition from the total reflection regime to the almost complete transparency regime (with a transparency coefficient of more than 50%) with varying plasma ion mass and/or laser pulse duration in the case of a fixed target thickness and electron density in it. These conclusions are important for the problems of 'light sail' laser-plasma ion acceleration, the optimum of which is achieved in targets with near-critical thicknesses.

Acknowledgements. The work was supported by the Ministry of Science and Higher Education of the Russian Federation within the State Assignment of the Lobachevsky State University of Nizhny Novgorod (Project No. 0729-2020-0035) and the Presidium of the Russian Academy of Sciences under the Research Programme 'Extreme light fields and their interaction with matter' (Project No. 0030-20190022). Numerical modelling was performed using resources provided by the Joint Supercomputer Centre of the Russian Academy of Sciences.

References

1. Korzhimanov A.V., Gonoskov A.A., Khazanov E.A., Sergeev A.M. *Phys. Usp.*, **54**, 9 (2011) [*Usp. Fiz. Nauk,* **181**, 9 (2011)].
2. Danson C., Hillier D., Hopps N., Neely D. *High Power Laser Sci. Eng.*, **3**, e3 (2015).
3. Gan Z. et al. *Opt. Express*, **25**, 5169 (2017).
4. Dollar F. et al. *Phys. Rev. Lett.*, **107**, 065003 (2011).
5. Dollar F. et al. *Phys. Plasmas*, **20**, 056703 (2013).
6. Green J.S. et al. *Appl. Phys. Lett.*, **104**, 214101 (2014).
7. Bychenkov V.Y. et al. *Phys. Plasmas*, **24**, 010704 (2017).
8. Nakatsutsumi M. et al. *Nat. Commun.*, **9**, 280 (2018).
9. Nishiuchi M. et al. *Phys. Plasmas*, **22**, 033107 (2015).
10. Faenov A.Ya. et al. *Sci. Rep.*, **5**, 13436 (2015).
11. Soloviev A. et al. *Sci. Rep.*, **7**, 12144 (2017).
12. Faenov A.Y. et al. *Appl. Phys. B: Lasers Opt.*, **123**, 1 (2017).
13. Henderson A. et al. *High Energy Density Phys.*, **12**, 46 (2014).
14. Wang H.Y., Liu B., Yan X.Q., Zepf M. *Phys. Plasmas*, **22**, 033102 (2015).
15. Liang E. et al. *Sci. Rep.*, **5**, 13968 (2015).
16. Yin L. et al. *Phys. Plasmas*, **14**, 056706 (2007).
17. Korzhimanov A.V., Gonoskov A.A., Kim A.V., Sergeev A.M. *JETP Lett.*, **86**, 577 (2008) [*Pis'ma Zh. Eksp. Teor. Fiz*, **86**, 662 (2007)].
18. Schlegel T. et al. *Phys. Plasmas*, **16**, 083103 (2009).
19. Robinson A.P.L., Kwon D.-H., Lancaster K. *Plasma Phys. Control. Fusion*, **51**, 095006 (2009).
20. Robinson A.P.L. *Phys. Plasmas*, **18**, 056701 (2011).
21. Korzhimanov A.V., Efimenko E.S., Golubev S.V., Kim A.V. *Phys. Rev. Lett.*, **109**, 245008 (2012).
22. Daido H., Nishiuchi M., Pirozhkov A.S. *Rep. Prog. Phys.*, **75**, 056401 (2012).
23. Macchi A., Borghesi M., Passoni M. *Rev. Mod. Phys.*, **85**, 58 (2013).
24. Bychenkov V.Yu., Brantov A.V., Govras E.A., Kovalev V.F. *Phys. Usp.*, **58**, 71 (2015) [*Usp. Fiz. Nauk*, **185**, 77 (2015)].
25. Akhiezer A.I., Polovin R.V. *Sov. J. Exp. Theor. Phys.*, **3**, 696 (1956) [*Zh. Exp. Teor. Fiz.*, **30**, 915 (1956)].
26. Lefebvre E., Bonnaud G. *Phys. Rev. Lett.*, **74**, 2002 (1995).
27. Cattani F., Kim A., Anderson D., Lisak M. *Phys. Rev. E*, **62**, 1234 (2000).
28. Siminos E. et al. *Phys. Rev. E*, **86**, 056404 (2012).
29. Eremin V.I., Korzhimanov A.V., Kim A.V. *Phys. Plasmas*, **17**, 043102 (2010).
30. Siminos E., Grech M., Svedung Wettervik B., Fülöp T. *New J. Phys.*, **19**, 123042 (2017).
31. Korzhimanov A.V., Eremin V.I., Kim A.V., Tushentsov R.M. *J. Exp. Theor. Phys.*, **105**, 675 (2007) [*Zh. Exp. Teor. Fiz.*, **132**, 771 (2007)].
32. Korzhimanov A.V., Efimenko E.S., Kim A.V., Golubev S.V. *Quantum Electron.*, **43**, 217 (2013) [*Kvantovaya Elektron.*, **43**, 217 (2013)].
33. Nerush E.N., Kostyukov I.Y., Ji L., Pukhov A. *Phys. Plasmas.*, **21**, 013109 (2014).
34. Macchi A., Cattani F., Liseykina T.V., Cornolti F. *Phys. Rev. Lett.*, **94**, 165003 (2005).
35. Surmin I.A. et al. *Comput. Phys. Commun.*, **202**, 204 (2016).
36. Vshivkov V.A., Naumova N.M., Pegoraro F., Bulanov S.V. *Phys. Plasmas.*, **5**, 2727 (1998).
37. Gonoskov A.A. et al. *Phys. Rev. Lett.*, **102**, 184801 (2009).